

VORTEX: Aligning Task Utility and Human Preferences through LLM-Guided Reward Shaping

Guojun Xiong*, Milind Tambe
Department of Computer Science, Harvard University
Cambridge, MA, USA
{gjxiong,tambe}@g.harvard.edu

Abstract

In social impact optimization, AI decision systems often rely on solvers that optimize well-calibrated mathematical objectives. However, these solvers cannot directly accommodate evolving human preferences, typically expressed in natural language rather than formal constraints. Recent approaches address this by using large language models (LLMs) to generate new reward functions from preference descriptions. While flexible, they risk sacrificing the system’s core utility guarantees. In this paper, we propose VORTEX, a language-guided reward shaping framework that preserves established optimization goals while adaptively incorporating human feedback. By formalizing the problem as multi-objective optimization, we use LLMs to iteratively generate shaping rewards based on verbal reinforcement and text-gradient prompt updates. This allows stakeholders to steer decision behavior via natural language without modifying solvers or specifying trade-off weights. We provide theoretical guarantees that VORTEX converges to Pareto-optimal trade-offs between utility and preference satisfaction. Empirical results in real-world allocation tasks demonstrate that VORTEX outperforms baselines in satisfying human-aligned coverage goals while maintaining high task performance. This work introduces a practical and theoretically grounded paradigm for human-AI collaborative optimization guided by natural language.

1 Introduction

Organizations across domains deploy AI systems to optimize resource allocation with mathematical objectives carefully designed through extensive stakeholder consultation and domain expertise [26]. For instance, public health programs allocate outreach calls to maximize patient engagement [18, 33], conservation organizations distribute protection resources to preserve biodiversity [10], and emergency response systems route aid to minimize harm [11]. These objectives often represent years of institutional learning and proven operational success.

However, real-world conditions evolve rapidly. Public health crises shift demographic priorities [4], environmental changes alter conservation needs [23], or community feedback reveals service gaps [2]. In response, program managers frequently need to adjust their allocation strategies—perhaps to "prioritize elderly patients more during flu season" or "increase coverage for underserved rural communities." Such preference adjustments reflect operational intuition and are naturally expressed in informal language rather than mathematical formulations, especially by decision-makers who lack technical expertise to modify complex optimization functions directly [8]. See Figure 1 for illustration.

This creates a fundamental tension. The existing solvers cannot directly handle the preferences and organizations are not supposed to simply abandon their carefully calibrated objectives, which embody

*Correspondence to Guojun Xiong <gjxiong@g.harvard.edu>.

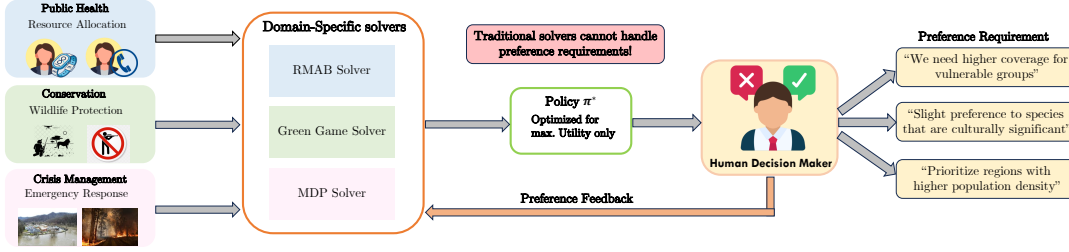


Figure 1: The fundamental tension between mathematical objective and human preferences.

substantial institutional knowledge and demonstrated performance. Yet ignoring evolving stakeholder preferences may lead to solutions that are mathematically optimal but operationally inadequate [22]. To bridge this tension, recent works [5, 28] generate entirely new reward functions from natural language descriptions with the aid of large language models (LLMs). While it enables flexible preference expression and maintains compatibility with existing solvers, it provides no guarantees about preserving performance on the original optimization criteria that organizations invested significant resources to develop.

This prompts us a question: how can we achieve mathematical optimality while respecting stakeholders' preferences?

To address this, we formulate a multi-objective optimization problem that preserves the established mathematical objective while incorporating human preferences as a second, alignment-oriented objective. A common technique is weighted scalarization [19, 25], which converts the problem into a single objective, and remains compatible with unmodified task-specific solvers. However, there remain two fundamental challenges. First, scalarization aims in navigating the Pareto frontier, which require users to specify explicit scalarization weights or engage in an iterative process of tuning these weights to explore the trade-off space, a significant burden for decision-makers who express preferences qualitatively. Second, these human preferences are often imprecise and expressed in natural language, making them difficult to encode as a formal mathematical objective [9].

To overcome these intertwined challenges, we propose VORTEX (Verbal-guided Optimization with Reward Tuning via Experiential Trajectory eXploration). To tackle the second challenge-encoding imprecise natural language preferences -VORTEX employs an LLM to generate auxiliary shaping rewards directly from this qualitative feedback. Crucially, to overcome the first challenge-navigating the Pareto frontier without the burden of manual weight tuning-VORTEX introduces an iterative framework that refines these shaping rewards through verbal reinforcement and text-gradient updates[35]. Rather than replacing carefully engineered objectives, our approach augments them with adaptive, preference-aligned signals, allowing stakeholders to steer decision behavior while using existing solvers unmodified. We further provide theoretical guarantees that this process converges to Pareto-optimal solutions, achieving a principled trade-off between task utility and preference satisfaction.

Our Contributions. We summarize our main contributions as follows.

▷ *New Problem Formulation:* We cast the challenge of aligning algorithmic decision-making with human preferences as a multi-objective optimization problem, preserving core task utility while introducing a separate preference satisfaction objective.

▷ *Solver-Compatible Reward Shaping:* We propose a novel framework that leverages LLMs to encode human preference objectives via reward shaping, enabling compatibility with unmodified, reward-driven solvers.

▷ *Interactive Preference Refinement:* We propose an iterative optimization procedure, VORTEX, that refines LLM prompts using verbal feedback and text-gradient updates to navigate the Pareto frontier between

task performance and preference alignment without specifying tradeoff weights.

▷ *Theoretical and Empirical Validation:* We prove that VORTEX converges to Pareto-optimal solutions under mild assumptions, and we demonstrate its effectiveness on real-world resource allocation tasks, achieving improved preference satisfaction while maintaining high task utility.

2 Related Work

Reward Shaping and Preference Constraints. Reward shaping is a long-standing technique in reinforcement learning (RL) [21] to accelerate learning or incorporate auxiliary objectives. Recent works study shaping for fairness [13], diversity [7], and coverage [27]. Our contribution lies in introducing an LLM-based mechanism to generate adaptive shaping signals from free-form natural language feedback, enabling soft and imprecise constraints to be expressed without formal modeling.

LLMs for Decision Optimization. Recent work explores how LLMs can assist in or automate decision-making tasks. For example, [32, 35] finetuned LLMs as proxy policy networks for conducting complex sequential decision-making tasks. Eureka [17] and Auto MC-Reward [16] has shown that LLMs can effectively generate reward functions from language specifications. Language to Rewards [34] trains LLMs to translate language instructions into reward functions for robotic tasks. [15] investigates the simplification of reward design via language interfaces, leveraging LLMs as proxy reward functions. The DLM framework [5, 28] uses LLMs to generate reward functions for resource allocation in public health settings. However, such approaches risk overriding core domain utility, as they optimize solely for human-specified preferences. Our framework complements this by integrating LLM-generated shaping rewards into an existing solver’s base reward, preserving task utility while iteratively improving preference alignment. Table 1 compares DLM with this paper from multiple dimensions.

Multi-objective and Constrained RL. Multi-objective RL [25] and constrained MDPs [3] offer formal treatments of utility trade-offs. A common technique is weighted scalarization [12, 19], which converts the multi-objective problem into a single objective. While foundational, a persistent challenge with scalarization lies in navigating the Pareto frontier, often requiring explicit scalarization weights or engaging in an iterative process of tuning these weights to explore the trade-off space. In contrast, VORTEX introduces a novel language-guided paradigm to navigate the Pareto frontier. It bypasses manual weight tuning by using an LLM to translate verbal feedback into adjustments to the shaping reward, making the process more intuitive and accessible.

Human-in-the-Loop Optimization. There is a rich literature on incorporating human preferences into algorithmic decision-making. Traditional methods include inverse RL [1, 20] and preference-based RL [9], where human feedback is used to infer or adapt the reward function. However, these methods typically require structured queries or labeled comparisons and are limited by scalability in real-world deployments. Our work instead leverages LLMs as flexible oracles for encoding natural language preferences into reward shaping, enabling rapid and adaptive preference integration without retraining policies.

3 Problem Formulation

3.1 Problem Statement

We consider a family of decision-making problems that can be formulated as constrained stochastic optimization, such as public health resource allocation or conservation planning. Formally, we define a population of N units (e.g., patients, species, or locations), each with a state $s_i(t) \in \mathcal{S}$, and an action

Table 1: We highlight the difference between our proposed method VORTEX and prior approaches. VORTEX uniquely supports multi-objective optimization, provides theoretical guarantees, and allows trade-off control—while prior methods either ignore base objectives, lack formal analysis, or offer limited preference alignment.

Method	Multiple Objective?	Entire Reward Generation?	Theoretical Guarantee?	Tradeoff Control?
Decision Language Model				
DLM [5]	✗	✓	✗	✗
SCLM [28]				
Conventional RL				
Eureka [17]	✗	✓	✗	✗
Auto-MC [16]				
VORTEX (proposed)	✓	✗	✓	✓

$a_i(t) \in \{0, 1\}$ at time t . Specifically, action $a_i(t) = 1$ represents the unit i is being allocated with a resource at time step t and action 0 otherwise. Let $P_i(s'|s, a)$ be the transition probability from state s to s' under action a for unit i . At each decision time slot, the decision maker can choose up to B units to interact, which leads to a global *budget constraint* restricts total interactions: $\sum_{i=1}^N a_i(t) \leq B, \quad \forall t$.

Task Utility. Let $R_{\text{base},i}(t)$ denote the task-defined reward for unit i at time t , which depends on the current state $s_i(t)$ and action $a_i(t)$, reflecting the intrinsic domain goal (e.g., a patient becoming adherent or a habitat improving). The cumulative task utility under any policy π is:

$$U(\pi) = \mathbb{E}_\pi \left[\sum_{t=1}^T \sum_{i=1}^N R_{\text{base},i}(t) \right]. \quad (1)$$

Hence, the goal is to find a policy π mapping states to actions such that it maximizes the expected cumulative reward under the given dynamics¹:

$$\max_{\pi \in \Pi_{\text{feasible}}} U(\pi), \quad (2)$$

where Π_{feasible} is the policy set that meets the interaction budget constraint $\sum_{i=1}^N a_i(t) \leq B, \quad \forall t$.

Preference satisfaction. Notice that each unit in the population is represented by a feature vector $z_i \in \mathcal{Z}$ capturing domain-specific attributes relevant to decision-making. In practice, human decision-makers often have additional soft or imprecise preference constraints that express high-level societal or ethical priorities, going beyond the base task utility maximization problem in (2). We provide a toy example to illustrate it as follows.

Example 1. Consider a public health planner allocating outreach calls to a population of pregnant women [18]. Each woman is described by a feature vector z_i consisting of: **Age**, **Education level**, and **Income level**, with each containing three levels, i.e., *Low*, *Medium*, *High*. For a feature vector $z_i = [100100100]$, it represents a "young low-education low-income" patient. Human decision-makers might require:

"Prioritize elderly patients slightly more than younger patients, even if it reduces short-term utility marginally."

¹The problem in (2) is a special case of the well-known restless multi-armed bandit problem [29], which can be solved by solvers in [18, 30, 31].

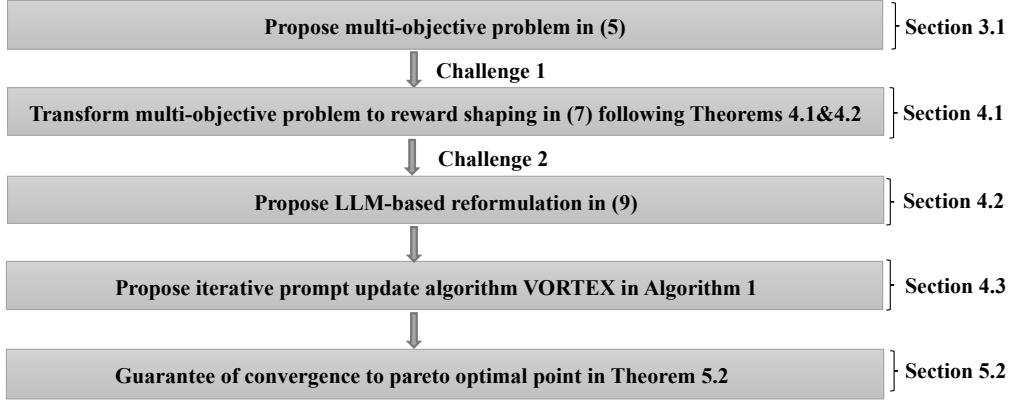


Figure 2: The main flow of contribution in this work.

The soft preference constraints are encoded as functions over the empirical feature visitation distribution for policy π :

$$D_\pi(z) = \frac{\# \text{ of units with feature } z \text{ being served}}{\# \text{ of total units being served}}. \quad (3)$$

Hence, it adds to a second-dimensional objective, i.e., achieving the desired demographic distribution

$$\min_{\pi \in \Pi_{feasible}} C(\pi) := \text{Div}(D_\pi, D_{\text{preference}}), \quad (4)$$

where $D_{\text{preference}}$ is the soft and imprecise preference constraint from human decision-makers, and Div is a general f -divergence measure.

Multi-objective Problem. Our goal is to find a policy π that simultaneously maximizes task utility $U(\pi)$ and minimizes preference deviation $C(\pi)$, with respect to the budget constraint $\sum_i a_i(t) \leq B$ for each t . This defines a multi-objective constrained optimization problem:

$$\max_{\pi \in \Pi_{feasible}} (U(\pi), -C(\pi)). \quad (5)$$

Pareto Frontier. The *Pareto frontier* $\mathcal{P} \subset \mathbb{R}^2$ of (5) is defined as:

$$\mathcal{P} := \left\{ (U(\pi), -C(\pi)) \left| \begin{array}{l} \nexists \pi' \in \Pi_{feasible} \text{ such that:} \\ U(\pi') \geq U(\pi), \\ -C(\pi') \geq -C(\pi) \end{array} \right. \right\}.$$

This set characterizes policies for which no other feasible solution simultaneously improves task utility and reduces preference violation. The set of all Pareto optimal solutions forms the Pareto frontier, representing all possible trade-offs between task utility and preference satisfaction.

Remark 1. Modeling human preferences as a separate optimization objective, rather than a hard constraint, offers three key advantages: it avoids feasibility issues from overly strict or conflicting constraints, enables transparent trade-offs between competing goals, and allows solution quality to be evaluated via Pareto optimality [25].

3.2 Challenges for (5)

Challenge 1: Navigating the Pareto Frontier. While weighted scalarization [19] allows us to combine task utility and preference satisfaction into a single objective, it requires a precise scalarization weight

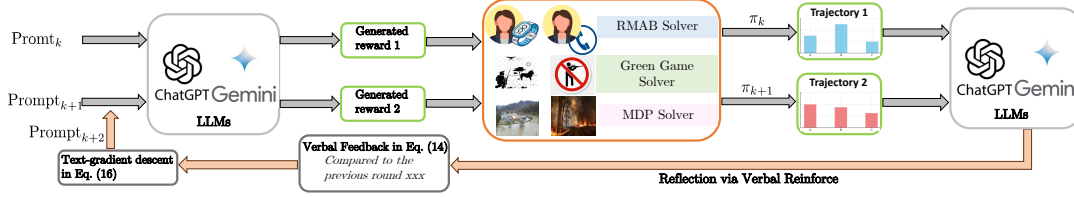


Figure 3: The detailed procedure of VORTEX. At each iteration, VORTEX compares two consecutive policy trajectories and reflects on their differences via verbal reinforcement. The resulting feedback is used to perform a text-gradient update on the LLM prompt, progressively refining the shaping reward to improve alignment.

specified to navigate the resulting Pareto frontier to find a solution that aligns with stakeholder preferences. This creates a significant practical barrier, often leading to a tedious trial-and-error process of tuning weights to explore the trade-off space. To bridge this gap, we draw on scalarization theory to transform preference alignment into a reward-shaping task. This allows us to encode human preferences as an auxiliary reward signal without tuning the weight. This full method is described Section 4.1.

Challenge 2: Imprecise human preferences. Human-specified preferences are typically high-level, and underspecified, without providing an exact quantitative target distribution. This makes the divergence objective (4) ill-defined. To address this, we propose to treat human preferences as latent objectives that can be implicitly captured through natural language by LLMs. In this way, the divergence term is approximated through LLM-based reward shaping and feedback, allowing us to integrate soft constraints into existing solvers without requiring formal definitions. This will be elaborated in Section 4.2. The main flow of contribution in this work is summarized in Figure 2.

4 Proposed Method: VORTEX

We begin by showing that the multi-objective problem in (5) can be equivalently reformulated as a reward shaping problem. We then recast it as a prompt optimization problem over LLM-generated shaping rewards. Finally, we present the full VORTEX algorithm and its iterative optimization procedure.

4.1 From Multi-objective to Reward Shaping

Provided the challenge that existing solvers fail for the multi-objective problem in (5), we leverage the scalarization theory [19] of multi-objective optimization to translate (5) into a reward shaping problem. Therefore, it maintains compatibility with existing solvers.

Scalarization Theory We establish the theoretical foundation for converting multi-objective optimization to reward shaping through the following theorem.

Theorem 2 (Weighted Scalarization[19]). *For the multi-objective problem defined in (5), a policy π^* is Pareto optimal if and only if there exists a weight $\lambda \in [0, 1]$ such that π^* is an optimal solution to the scalarized problem:*

$$\max_{\pi} J_{\lambda}(\pi) = \lambda U(\pi) - (1 - \lambda)C(\pi). \quad (6)$$

We now show how the scalarized objective can be reformulated as a reward shaping problem in the following theorem.

Theorem 3 (Multi-objective to Reward Shaping). *The scalarized multi-objective problem is equivalent to optimizing a single objective with shaped rewards:*

$$\max_{\pi} J_{\lambda}(\pi) = \mathbb{E}_{\pi} \left[\sum_{i=1}^N \sum_{t=1}^T R_{shaped,i}(s_i(t), a_i(t), z_i) \right], \quad (7)$$

where the shaped reward is defined as:

$$R_{shaped,i}(s, a, z_i) = R_{base,i}(s, a) + R_h(z_i), \quad (8)$$

with shaping reward being $R_h(z) \propto \frac{1-\lambda}{\lambda} \cdot \frac{\partial}{\partial D_{\pi}(z)} \text{Div}(D_{\pi} \| D_{preference})$.

Corollary 1 (Parameter Interpretation). *The scalarization parameter λ has the following interpretation: 1) $\lambda \rightarrow 1$: focus primarily on task utility; 2) $\lambda \rightarrow 0$: focus primarily on preference satisfaction.*

Remark 4. The key insight is that the shaping reward $R_h(z)$ depends on how far the current feature distribution $D_{\pi}(z)$ deviates from the preference distribution, adjusted by the relative importance weights. In practice, this theoretical form guides the LLM’s reward generation through natural language feedback.

This theoretical framework establishes that any Pareto optimal solution to the multi-objective problem can be found by solving a single-objective problem with appropriately shaped rewards, providing the mathematical foundation for our approach in Section 4.2.

4.2 LLM-based Reformulation of (5)

According to Theorem 3, the multi-objective optimization problem can be addressed through appropriate reward shaping. To tackle the second challenge, we therefore propose a novel framework that enables LLMs to generate an auxiliary reward term R_h , shifting the focus to prompt optimization for producing high-quality, preference-aligned shaping rewards.

Joint Optimization Objective. Let `Prompt` denote the input to the LLM, consisting of a fixed task description and an adaptive feedback component that evolves over time. Given `Prompt`, the LLM generates a shaping reward vector R_h , which is combined with the base reward and passed to a solver to produce a policy π . As a result, the original multi-objective problem in (5) can be reformulated as:

$$\begin{aligned} \max_{\text{Prompt}} & \left(\underbrace{U(\pi)}_{\text{task utility}}, - \underbrace{C(\pi, R_h)}_{\text{preference violation}} \right) \\ \text{s.t. } & R_h = \text{LLM}(\text{Prompt}), \pi = \text{Solver}(R_{\text{base}} + R_h). \end{aligned} \quad (9)$$

Here, $C(\pi, R_h)$ measures the divergence between the state-feature visitation distribution induced by policy π and the desired preference pattern (e.g., demographic fairness), and the solver obeys all operational constraints, such as budget.

Solver and Reward Composition. Given a reward function combining base and shaped components, the solver optimizes the policy under feasibility constraints:

$$\pi = \arg \max_{\pi \in \Pi_{\text{feasible}}} \mathbb{E}_{\pi} \left[\sum_{t=1}^T \sum_{i=1}^N (R_{\text{base},i}(t) + R_h(z_i)) \right]. \quad (10)$$

Pareto Frontier Navigation Via Language Models. Rather than manually tuning scalarization weights (e.g., Lagrange multipliers), our framework leverages LLMs to shape rewards through iterative natural

language reflection. In the formulation (9), the LLM serves as a bridge between human intent and formal optimization, translating imprecise preferences into a shaped reward R_h that complements the base objective. By iteratively refining R_h based on observed trade-offs between utility U and preference violation C , the framework progressively steers the policy toward better alignment along the Pareto frontier. See Figure 7 for an illustration.

Table 2: Comparison of consecutive trajectories and feature-specific reward adjustment suggestions in the public health domain.

Metric	Episode k	Episode $k + 1$	Change
Utility	82.4	80.7	-1.7
Coverage	22.0%	27.5%	+5.5%
Verbal Feedback: “Compared to the previous round, reward decreased slightly (-1.7), but coverage improved (+5.5%). To further improve alignment: (1) Increase shaping reward for patients under age 25 ; (2) Decrease shaping reward for patients over age 60 , who are frequently selected but yield no benefit;			

4.3 VORTEX: Description

Our proposed method, VORTEX, is an iterative algorithm that refines the LLM-generated shaping reward, R_h , through a closed loop of generation, execution, and reflection. The goal is to progressively steer the system’s policy toward a desirable point on the Pareto frontier of task utility and preference satisfaction. The core of VORTEX is an iterative process where each step builds upon the last. At each episode k , the algorithm executes four main steps: (1) Reward Generation, (2) Policy Execution and Evaluation, (3) Verbal Reinforcement via Reflection, and (4) Text-Gradient Prompt Optimization. This entire workflow is illustrated in Figure 3.

Step 1: LLM-Powered Reward Generation. Each episode begins by constructing a prompt, Prompt_k as

Task: Generate a shaping reward vector to encourage slightly higher coverage for demographic group X while preserving high total reward.
Context: Each arm has state s_i and features z_i .
Reflection: Previous round achieved xx% of max reward but only xx% coverage for group G.
Instruction: Assign additional reward values to each arm to improve group G coverage with minimal reward loss.
Output: A reward function R_h representing the preference-aligned shaping reward.

The LLM processes this comprehensive prompt to generate a new shaping reward,

$$R_h^k = \text{LLM}(\text{Prompt}_k). \quad (11)$$

Step 2: Policy Execution and Evaluation. The generated shaping reward, R_h^k , is added to the base task reward, R_{base} . This combined reward function is then passed to the pre-existing, unmodified domain-specific solver. The solver, operating under its constraints (e.g., budget B), calculates the optimal policy π_k . This policy is then deployed in the environment to collect a trajectory,

$$\tau^k = \{(s_i(t), a_i(t), z_i, R_{\text{base},i}(t)), \forall i\}_{t=1}^T.$$

Let the previous trajectory be τ^{k-1} , obtained from policy π^{k-1} . For both trajectories, we compute the total expected reward

$$U_k = \mathbb{E}_{\pi^k} \left[\sum_{t=1}^T \sum_i R_{\text{base},i}(t) \right], \quad (12)$$

and empirical feature distribution

$$D_k(z) = \frac{\# \text{ of unit with feature } z \text{ being served}}{\# \text{ of total units being served}}. \quad (13)$$

Step 3: Verbal Reinforcement via Trajectory Comparison. This step serves as the reflective engine of VORTEX. It synthesizes performance changes into structured, actionable feedback. The system compares the metrics from the current trajectory τ^k with the previous one τ^{k-1} by computing changes across iterations:

$$\delta_U = U_k - U_{k-1}, \quad \delta_D = D_k(z) - D_{k-1}(z). \quad (14)$$

This quantitative comparison is then translated into qualitative, natural language feedback, which we term Verbal Reinforcement. This can be handled by a function or a separate LLM call,

$$\text{Feedback}_{\text{verbal}}^k = f(\delta_U, \delta_D). \quad (15)$$

The feedback explicitly states the trade-off that was observed and provides concrete suggestions for the next iteration. An example of this generated feedback is shown in Table 2.

Step 4: Text-Gradient Prompt Optimization In classical reinforcement learning, policies are updated via gradient descent $\theta \leftarrow \theta - \eta \nabla_{\theta} J(\theta)$. In our framework, we operate in the space of prompts rather than parameters. We decompose the prompt into two disjoint components:

$$\text{Prompt}_k = P_{\text{Fix}} \parallel P_{\text{Editable},k}, \quad (16)$$

where P_{Fix} contains static information about the task, input format, and solver API that remains unchanged across iterations, and $P_{\text{Editable},k}$ is the dynamic portion, refined at each step using semantic feedback. The update rule mimics gradient-based optimization but operates in the space of text. The verbal feedback from Step 3 serves as the "text-gradient," which is appended to the editable portion of the prompt:

$$P_{\text{Editable},k+1} \leftarrow P_{\text{Editable},k} + \text{Feedback}_{\text{verbal}}^k, \quad (17)$$

and construct the new prompt as:

$$\text{Prompt}_{k+1} = P_{\text{Fix}} \parallel P_{\text{Editable},k+1}. \quad (18)$$

This updated prompt, now containing a historical account of what has been tried and a clear directive for what to do next, is fed to the LLM in the next iteration (Step 1). This iterative refinement loop, summarized in Algorithm 1, continues until a satisfactory trade-off between utility and preference satisfaction is achieved or a set number of episodes is completed.

Remark 5. Our framework treats the LLM as an adaptive reward generator, using trajectory-level comparisons to produce verbal feedback that acts as a soft "gradient" in prompt space. This enables iterative refinement of shaping rewards toward better utility-preference trade-offs, without requiring to specify trade-off weights in [12].

Remark 6 (Multi-Run Pareto Exploration). While each execution of VORTEX converges to a single Pareto-optimal point (Theorem 7 in Section 5), stakeholders may wish to explore different trade-offs between task utility and preference satisfaction. Our framework naturally supports this through multiple runs, where each iteration is conditioned on feedback from the previous result. If stakeholders find the current balance unsatisfactory—for instance, preferring higher coverage despite reduced efficiency—they can provide directional feedback that guides the next run toward a different region of the Pareto frontier. This iterative refinement process allows practical navigation of trade-offs without requiring explicit weight specification.

Algorithm 1: VORTEX: Verbal-guided Optimization with Reward Tuning via Experiential Trajectory Exploration

Require: Initial Prompt₀, task domain, base reward R_{base} , budget B , number of episodes K ;

- 1: Initialize $\tau^{-1} \leftarrow$ random baseline (or empty trajectory)
 - 2: **for** $k = 0$ to $K - 1$ **do**
 - 3: **(LLM)** Generate shaping reward R_h^k following (11);
 - 4: **(Solver)** Solve policy π^k according to (10);
 - 5: **(Execute)** Deploy π^k in \mathcal{E} to collect trajectory τ^k ;
 - 6: **(Compute)** Evaluate task utility U_k in (12) and feature distribution $D_k(z)$ in (13);
 - 7: **if** $k > 0$ **then**
 - 8: **(Compare)** Compute difference: δ_U, δ_Δ in (14) ;
 - 9: **(Feedback)** Generate verbal reflection by (15);
 - 10: **(Text-Gradient)** Update prompt based on (18);
 - 11: **end if**
 - 12: **end for**
 - 13: **Return:** Final Prompt _{K} , policy π^K ;
-

5 Theoretical Guarantee

We analyze the convergence properties of our iterative framework VORTEX. The key challenge is that we are optimizing in the space of reward shaping functions to explore the Pareto frontier. We first make some necessary assumptions, and then present the main result.

5.1 Convergence Analysis

Assumption 1. *We make the following assumptions:*

1. **(A1) Solver Optimality:** *For given shaping reward R_h , the external solver returns globally optimal policy $\pi^*(R_h)$.*
2. **(A2) Preference Convexity:** *The divergence term $C(\pi)$ is convex with respect to the feature distribution.*
3. **(A3) Text-Gradient Quality:** *The verbal reinforcement provides an unbiased (or bounded-bias) stochastic estimate of gradient $\nabla_{R_h}[J_\lambda(R_h)]$ with bounded variance.*

Assumption (A1) abstracts away the complexity of the underlying optimization problem by treating the solver as a reliable oracle, realistic in many applications. It allows us to focus the analysis on the behavior of the LLM-driven reward shaping mechanism rather than solver errors. Assumption (A2) ensures the existence of gradients and well-behaved optimization landscape, which can be easily satisfied when f -divergence is KL-divergence or total variation. Assumption (A3) is the most critical, requiring that LLM feedback provides meaningful directional information with vanishing bias, which is supported by the structured nature of trajectory comparisons.

5.2 Main Result

Theorem 7 (Convergence to Pareto Optimal Point). *If the LLM’s preference encoding corresponds to some implicit scalarization weight λ , under Assumptions (A1)–(A3), the proposed iterative VORTEX converges almost surely to a stationary point R_h^* such that the resulting policy $\pi^*(R_h^*)$ achieves a Pareto optimal trade-off:*

$$\left(U(R_h^*) = \mathbb{E}_{\pi^*(R_h^*)}[R_{\text{base}}], C(R_h^*) = -C(\pi^*(R_h^*)) \right) \in \mathcal{P}.$$

Proof Sketch. Our proof sketch involves three main parts. We begin by reformulating the bi-objective problem as a single, differentiable scalarized objective. We then use stochastic approximation theory to relate our algorithm’s discrete update rule to a continuous-time ODE. Finally, we use a Lyapunov-based analysis to show that the ODE converges to stationary points, and we prove these points are Pareto-optimal solutions to the original problem, guaranteeing convergence. Detailed proof can be found in Appendix B in the supplementary materials. \square

Remark 8. Our convergence analysis offers several key takeaways: Under mild assumptions, the iterative procedure converges to a fixed point where the LLM no longer modifies its shaping reward; The converged solution lies on the Pareto frontier, achieving a balance between task utility and human preference satisfaction.

6 Experiments

To evaluate VORTEX, we simulate a constrained public health intervention scenario inspired by the ARMMAN maternal health setting [5, 18] and a conservation setting [24]. For fair comparison with SOTA baseline DLM in [5], we use Gemini-2.5-Pro as the LLM in our experiments. We present the main results for the public health domain in this section, and detailed setting descriptions and more results can be found in Appendix C in the supplementary materials.

Environment abstract. We simulate a population of 800 mothers, evenly partitioned into 8 demographic types based on three binary features: **Income:** Low / High; **Education:** Low / High; **Age:** Young / Old. At each round, the planner is allowed to intervene with up to $B = 400$ mothers. **Preference requirement:** The human decision-maker specifies a soft equity preference such as: “*Slightly prefer mothers with specific features, such as low income, low education, young age.*” In this simulation, we consider 6 different preferences as favor high/low income(HI/LI), high/low education (HE/LE), Old, and Young.

6.1 Results

Effectiveness of Reward Shaping. The effectiveness of the proposed reward shaping technique is evaluated by visualizing the trade-off between task utility and human preference satisfaction.

As shown in Figure 4, the "Base Reward" policy, optimized solely for utility, achieves the highest performance with a median reward of approximately 432. As soon as any human preference is introduced via reward shaping, total utility declines. This result highlights the inherent cost of alignment, demonstrating that satisfying qualitative preferences requires a trade-off with the unconstrained performance metric.

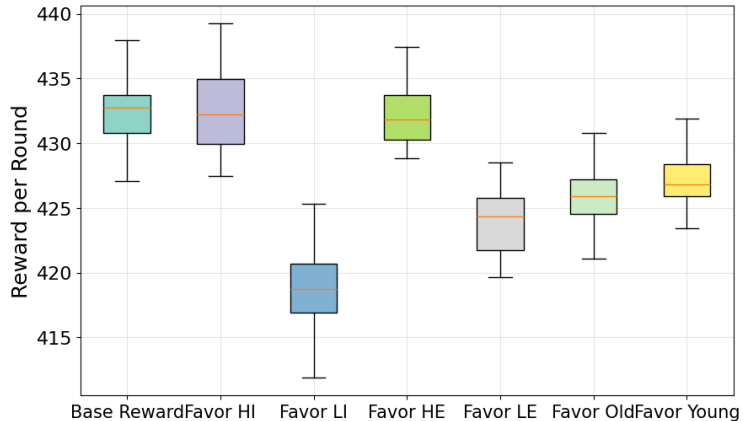


Figure 4: Reward comparison.

Figure 5 illustrates the success of reward shaping in enforcing preferences. While the "Base Reward" policy is clearly biased (e.g., allocating resources 0.78 to high-income vs. 0.22 to low-income individuals),

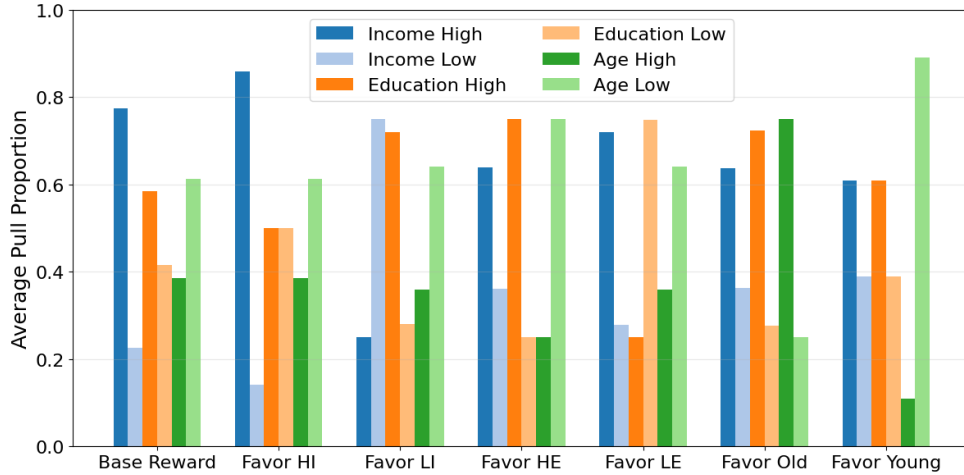


Figure 5: Coverage ratio comparison.

this is effectively corrected when a preference is applied. For instance, under the "Favor LI" condition, the pull proportion for LI individuals substantially increases to 0.75. This successful shift towards the targeted group is observed across all tested preference conditions.

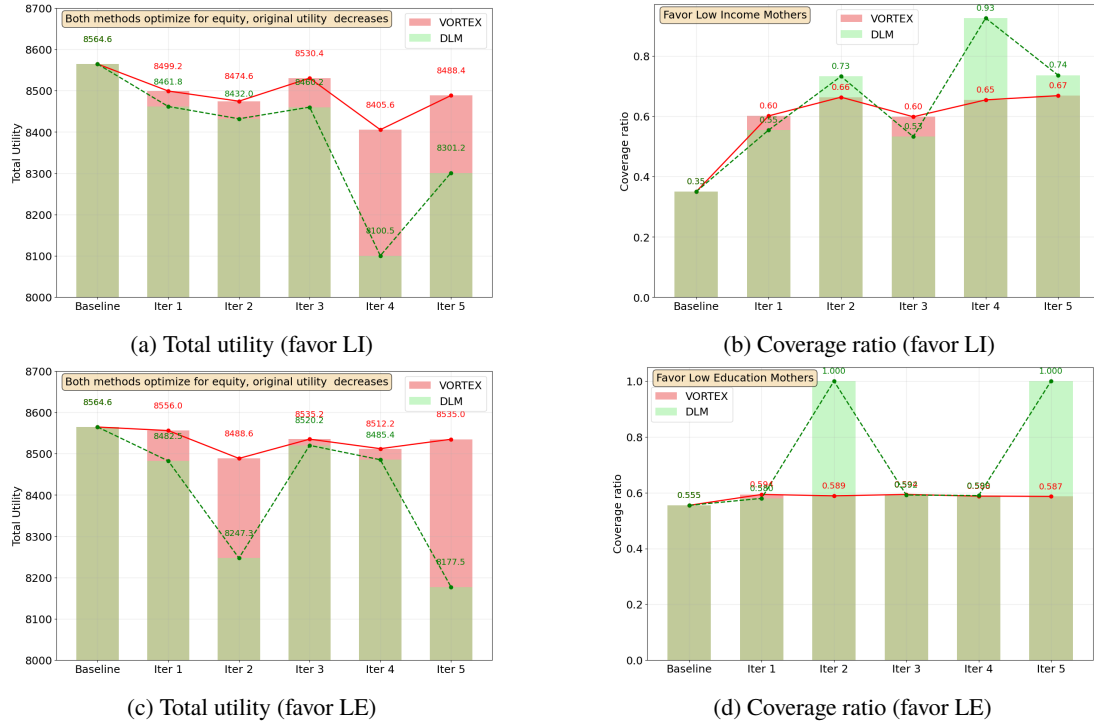


Figure 6: Comparison with DLM for ARMMAN.

Baseline comparison. Figure 19 presents a comparison between our proposed VORTEX, against the SOTA baseline, DLM. The comparison is conducted over five iterative rounds, evaluating both total utility and the coverage ratio for two specified human preferences ("Favor LI" and "Favor LE"). More experiments are relegated to Appendix C.

Figures 12a and 19a compare the total utility. VORTEX maintains a high and stable utility after a controlled initial drop, while the DLM baseline is highly volatile and suffers a dramatic drop in utility during its run.

This highlights VORTEX’s ability to incorporate human preferences without the excessive performance cost and instability exhibited by DLM. Figures 12b and 19b show the coverage ratio for the targeted "low income" group, highlighting the different trade-offs made by each method. VORTEX achieves a steady and stable increase in coverage throughout the iterations. In contrast, DLM’s coverage is highly unstable, with erratic fluctuations and a high peak that corresponds to its utility collapse. VORTEX demonstrates a more balanced and reliable performance, substantially improving coverage while preserving high utility.

Pareto front navigation. Figure 7 visualizes how VORTEX navigates the Pareto front, illustrating the trade-off between Task Utility and Preference Satisfaction. It shows two distinct trajectories (T1 and T2) that start from a shared, high-utility baseline. As the iterations progress, both trajectories sacrifice utility to gain preference satisfaction, each exploring a different region of the solution space. Both runs demonstrate clear convergence, settling on different final solutions: T1 favors a higher utility, while T2 prioritizes preference satisfaction. This highlights the framework’s ability to converge to stable, well-balanced solutions at different points on the Pareto frontier, catering to varying stakeholder priorities.

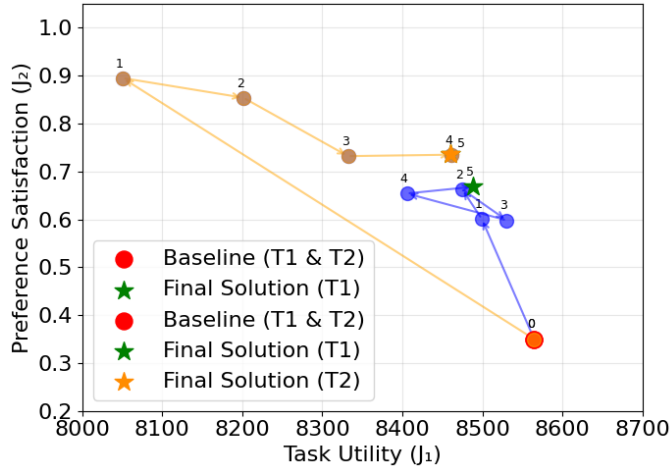


Figure 7: Pareto navigation.

7 Conclusion

We introduce VORTEX, a theoretically-grounded framework that uses an LLM to iteratively shape rewards, enabling a stable, Pareto-optimal balance between task utility and human language preferences without modifying existing solvers. We prove VORTEX converges to Pareto-optimal solutions and show it empirically outperforms baselines by achieving a more reliable and balanced performance.

References

- [1] Pieter Abbeel and Andrew Y Ng. Apprenticeship learning via inverse reinforcement learning. In *Proceedings of the 21st International Conference on Machine Learning*, 2004.
- [2] Rediet Abebe, Solon Barocas, Jon Kleinberg, Karen Levy, Manish Raghavan, and David G Robinson. Roles for computing in social change. In *Proceedings of the 2020 conference on fairness, accountability, and transparency*, pages 252–260, 2020.
- [3] Eitan Altman. *Constrained Markov Decision Processes*. Chapman and Hall/CRC, 1999.
- [4] Clare Bamba, Ryan Riordan, John Ford, and Fiona Matthews. The covid-19 pandemic and health inequalities. *J Epidemiol Community Health*, 74(11):964–968, 2020.
- [5] Nikhil Behari, Edwin Zhang, Yunfan Zhao, Aparna Taneja, Dheeraj Nagaraj, and Milind Tambe. A decision-language model (dlm) for dynamic restless multi-armed bandit tasks in public health. *arXiv preprint arXiv:2402.14807*, 2024.
- [6] Vivek S Borkar and Vivek S Borkar. *Stochastic approximation: a dynamical systems viewpoint*, volume 100. Springer, 2008.

- [7] L Elisa Celis, Lingxiao Huang, Vijay Keswani, and Nisheeth K Vishnoi. Classification with fairness constraints: A meta-algorithm with provable guarantees. In *Conference on Fairness, Accountability, and Transparency*, 2019.
- [8] Alexandra Chouldechova and Aaron Roth. The frontiers of fairness in machine learning. *arXiv preprint arXiv:1810.08810*, 2018.
- [9] Paul Christiano, Jan Leike, Tom Brown, Miljan Martic, Shane Legg, and Dario Amodei. Deep reinforcement learning from human preferences. In *Advances in Neural Information Processing Systems*, 2017.
- [10] Bistra Dilkina, Rachel Houtman, Carla P Gomes, Claire A Montgomery, Kevin S McKelvey, Katherine Kendall, Tabitha A Graves, Richard Bernstein, and Michael K Schwartz. Trade-offs and efficiencies in optimal budget-constrained multispecies corridor networks. *Conservation Biology*, 31(1):192–202, 2017.
- [11] Frank Fiedrich, Fritz Gehbauer, and Uwe Rickers. Optimized resource allocation for emergency response after earthquake disasters. *Safety science*, 35(1-3):41–57, 2000.
- [12] Conor F Hayes, Roxana Rădulescu, Eugenio Bargiacchi, Johan Källström, Matthew Macfarlane, Mathieu Reymond, Timothy Verstraeten, Luisa M Zintgraf, Richard Dazeley, Fredrik Heintz, et al. A practical guide to multi-objective reinforcement learning and planning. *Autonomous Agents and Multi-Agent Systems*, 36(1):26, 2022.
- [13] Shahin Jabbari, Matthew Joseph, Michael Kearns, Jamie Morgenstern, and Aaron Roth. Fairness in reinforcement learning. In *International Conference on Machine Learning*, 2017.
- [14] Harold Joseph Kushner and Dean S Clark. *Stochastic approximation methods for constrained and unconstrained systems*, volume 26. Springer Science & Business Media, 2012.
- [15] Minae Kwon, Sang Michael Xie, Kalesha Bullard, and Dorsa Sadigh. Reward design with language models. *arXiv preprint arXiv:2303.00001*, 2023.
- [16] Hao Li, Xue Yang, Zhaokai Wang, Xizhou Zhu, Jie Zhou, Yu Qiao, Xiaogang Wang, Hongsheng Li, Lewei Lu, and Jifeng Dai. Auto mc-reward: Automated dense reward design with large language models for minecraft. In *Proceedings of the IEEE/CVF Conference on Computer Vision and Pattern Recognition*, pages 16426–16435, 2024.
- [17] Yecheng Jason Ma, William Liang, Guanzhi Wang, De-An Huang, Osbert Bastani, Dinesh Jayaraman, Yuke Zhu, Linxi Fan, and Anima Anandkumar. Eureka: Human-level reward design via coding large language models. *arXiv preprint arXiv:2310.12931*, 2023.
- [18] Aditya Mate, Lovish Madaan, Aparna Taneja, Neha Madhiwalla, Shresth Verma, Gargi Singh, Aparna Hegde, Pradeep Varakantham, and Milind Tambe. Field study in deploying restless multi-armed bandits: Assisting non-profits in improving maternal and child health. In *Proceedings of the AAAI Conference on Artificial Intelligence*, volume 36, pages 12017–12025, 2022.
- [19] Kaisa Miettinen. *Nonlinear multiobjective optimization*, volume 12. Springer Science & Business Media, 2012.
- [20] Andrew Y Ng and Stuart J Russell. Algorithms for inverse reinforcement learning. In *Proceedings of the 17th International Conference on Machine Learning*, 2000.
- [21] Andrew Y Ng, Daishi Harada, and Stuart J Russell. Policy invariance under reward transformations: Theory and application to reward shaping. In *International Conference on Machine Learning*, 1999.
- [22] Ziad Obermeyer, Brian Powers, Christine Vogeli, and Sendhil Mullainathan. Dissecting racial bias in an algorithm used to manage the health of populations. *Science*, 366(6464):447–453, 2019.

- [23] Robert L Pressey, Mar Cabeza, Matthew E Watts, Richard M Cowling, and Kerrie A Wilson. Conservation planning in a changing world. *Trends in ecology & evolution*, 22(11):583–592, 2007.
- [24] Yundi Qian, Chao Zhang, Bhaskar Krishnamachari, and Milind Tambe. Restless poachers: Handling exploration-exploitation tradeoffs in security domains. In *Proceedings of the 2016 International Conference on Autonomous Agents & Multiagent Systems*, pages 123–131, 2016.
- [25] Diederik M Roijers, Peter Vamplew, Shimon Whiteson, and Richard Dazeley. A survey of multi-objective sequential decision-making. *Journal of Artificial Intelligence Research*, 2013.
- [26] Zheyuan Ryan Shi, Claire Wang, and Fei Fang. Artificial intelligence for social good: A survey. 2020.
- [27] Shreya Venkataraman et al. Conservative fairness approaches for policy learning. In *Advances in Neural Information Processing Systems*, 2021.
- [28] Shresth Verma, Niclas Boehmer, Ling kai Kong, and Milind Tambe. Balancing act: Prioritization strategies for llm-designed restless bandit rewards. *arXiv preprint arXiv:2408.12112*, 2024.
- [29] Peter Whittle. Restless bandits: Activity allocation in a changing world. *Journal of applied probability*, 25(A):287–298, 1988.
- [30] Guojun Xiong, Jian Li, and Rahul Singh. Reinforcement learning augmented asymptotically optimal index policy for finite-horizon restless bandits. In *Proceedings of the AAAI Conference on Artificial Intelligence*, volume 36, pages 8726–8734, 2022.
- [31] Guojun Xiong, Shufan Wang, and Jian Li. Learning infinite-horizon average-reward restless multi-action bandits via index awareness. *Advances in Neural Information Processing Systems*, 35: 17911–17925, 2022.
- [32] Guojun Xiong, Zhiyang Deng, Keyi Wang, Yupeng Cao, Haohang Li, Yangyang Yu, Xueqing Peng, Mingquan Lin, Kaleb E Smith, Xiao-Yang Liu, et al. Flag-trader: Fusion llm-agent with gradient-based reinforcement learning for financial trading. *arXiv preprint arXiv:2502.11433*, 2025.
- [33] Guojun Xiong, Haichuan Wang, Yuqi Pan, Saptarshi Mandal, Sanket Shah, Niclas Boehmer, and Milind Tambe. Finite-horizon single-pull restless bandits: An efficient index policy for scarce resource allocation. *arXiv preprint arXiv:2501.06103*, 2025.
- [34] Wenhao Yu, Nimrod Gileadi, Chuyuan Fu, et al. Language to rewards for robotic skill synthesis. In *Conference on Robot Learning*, 2023.
- [35] Yangyang Yu, Zhiyuan Yao, Haohang Li, Zhiyang Deng, Yuechen Jiang, Yupeng Cao, Zhi Chen, Jordan Suchow, Zhenyu Cui, Rong Liu, et al. Fincon: A synthesized llm multi-agent system with conceptual verbal reinforcement for enhanced financial decision making. *Advances in Neural Information Processing Systems*, 37:137010–137045, 2024.

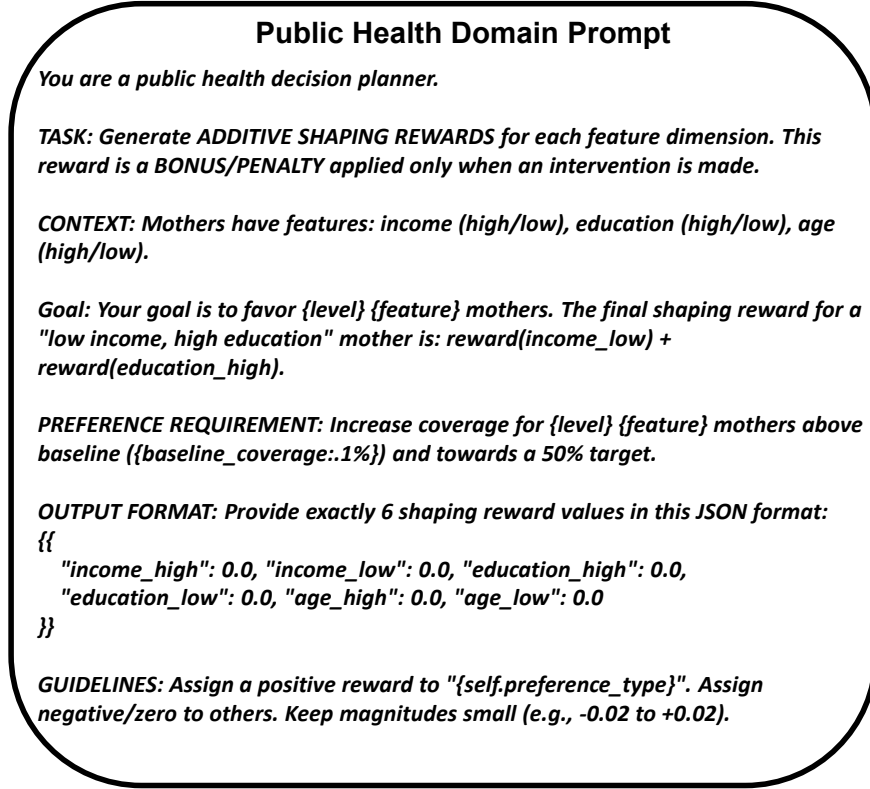


Figure 8: Prompt for VORTEX in public health domain.

A Missing Details

We provide the prompt example for the Public Health domain in Figure 8 and the associated VORTEX output in Figure 9.

B Technique Proofs

In this section, we provide detailed proofs for the theoretical results in the main paper.

B.1 Proof of Theorem 2

Necessity: Suppose π^* is Pareto optimal but not optimal for any scalarized problem. Then for all $\lambda \in [0, 1]$, there exists π_λ such that $J_\lambda(\pi_\lambda) > J_\lambda(\pi^*)$. This implies:

$$\lambda U(\pi_\lambda) - (1 - \lambda)C(\pi_\lambda) > \lambda U(\pi^*) - (1 - \lambda)C(\pi^*). \quad (19)$$

By the separating hyperplane theorem, since π^* is Pareto optimal, there exists $\lambda^* \geq 0$ such that no policy can simultaneously improve both objectives, contradicting the assumption.

Sufficiency: Suppose π^* is optimal for the scalarized problem with weight $\lambda > 0$. If π^* is not Pareto optimal, then there exists π' such that $U(\pi') \geq U(\pi^*)$ and $-C(\pi') \geq -C(\pi^*)$ with at least one strict inequality. This implies:

$$\lambda U(\pi') - (1 - \lambda)C(\pi') > \lambda U(\pi^*) - (1 - \lambda)C(\pi^*), \quad (20)$$

contradicting the optimality of π^* for the scalarized problem. This completes the proof.

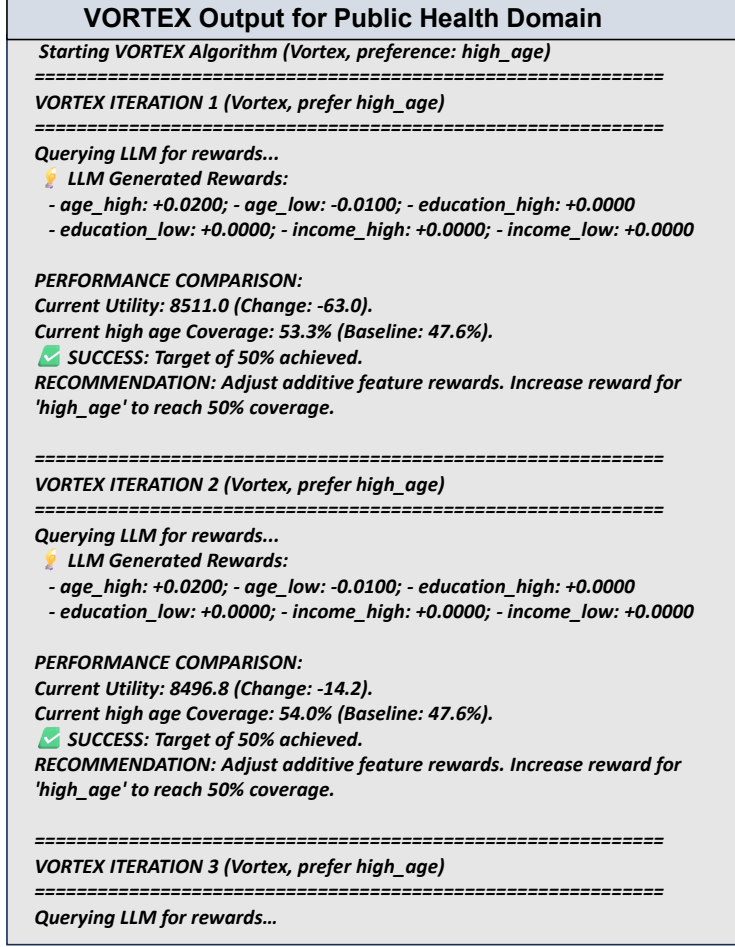


Figure 9: VORTEX output for public health domain

B.2 Proof of Theorem 3

Starting from the scalarized multi-objective problem in Theorem 2, we have

$$\begin{aligned}
J_\lambda(\pi) &= \lambda U(\pi) - (1 - \lambda)C(\pi) \\
&= \lambda \mathbb{E}_\pi \left[\sum_{t=1}^T \sum_{i=1}^N R_{\text{base},i}(s_i(t), a_i(t)) \right] - (1 - \lambda) \text{Div}(D_\pi \| D_{\text{preference}}). \tag{21}
\end{aligned}$$

For the f -divergence term, we have

$$\text{Div}(D_\pi \| D_{\text{preference}}) = \int f \left(\frac{dD_\pi}{dD_{\text{preference}}} \right) dD_{\text{preference}} = \sum_{z \in \mathcal{Z}} f \left(\frac{D_\pi(z)}{D_{\text{preference}}(z)} \right) D_{\text{preference}}(z), \tag{22}$$

where $D_\pi(z)$ is the empirical feature distribution under policy π

$$D_\pi(z) = \frac{\sum_{t=1}^T \sum_{i=1}^N \mathbb{1}(z_i = z) \cdot a_i(t)}{\sum_{t=1}^T \sum_{i=1}^N a_i(t)}. \tag{23}$$

Taking the partial derivative of the divergence with respect to $D_\pi(z)$

$$\frac{\partial}{\partial D_\pi(z)} \text{Div}(D_\pi \| D_{\text{preference}}) = \frac{\partial}{\partial D_\pi(z)} \sum_{z' \in \mathcal{Z}} f \left(\frac{D_\pi(z')}{D_{\text{preference}}(z')} \right) D_{\text{preference}}(z')$$

$$\begin{aligned}
&= f' \left(\frac{D_\pi(z)}{D_{\text{preference}}(z)} \right) \cdot \frac{1}{D_{\text{preference}}(z)} \cdot D_{\text{preference}}(z) \\
&= f' \left(\frac{D^\pi(z)}{D_{\text{preference}}(z)} \right).
\end{aligned} \tag{24}$$

The difference in feature distributions can be written as:

$$D_{\pi'}(z) - D_\pi(z) = \frac{\mathbb{E}_{\pi'} \left[\sum_{t,i:z_i=z} a_i(t) \right]}{\mathbb{E}_{\pi'} \left[\sum_{t,i} a_i(t) \right]} - \frac{\mathbb{E}_\pi \left[\sum_{t,i:z_i=z} a_i(t) \right]}{\mathbb{E}_\pi \left[\sum_{t,i} a_i(t) \right]}.$$
 \tag{25}

Since $\mathbb{E}_{\pi'}[\sum_{t,i} a_i(t)] \approx \mathbb{E}_\pi[\sum_{t,i} a_i(t)] = BT$, we have

$$\begin{aligned}
D_{\pi'}(z) - D_\pi(z) &= \frac{1}{BT} \left(\mathbb{E}_{\pi'} \left[\sum_{t,i:z_i=z} a_i(t) \right] - \mathbb{E}_\pi \left[\sum_{t,i:z_i=z} a_i(t) \right] \right) \\
&= \frac{1}{BT} \mathbb{E}_{\pi'} \left[\sum_{t=1}^T \sum_{i:z_i=z} a_i(t) \right] + \text{const.}
\end{aligned} \tag{26}$$

Hence, following first-order Taylor approximation, we have

$$\begin{aligned}
\text{Div}(D_{\pi'} \| D_{\text{preference}}) &\approx \text{Div}(D_\pi \| D_{\text{preference}}) + \sum_z f' \left(\frac{D_\pi(z)}{D_{\text{preference}}(z)} \right) \cdot \frac{1}{BT} \mathbb{E}_{\pi'} \left[\sum_{t=1}^T \sum_{i:z_i=z} a_i(t) \right] + \text{const} \\
&= \text{const} + \frac{1}{BT} \mathbb{E}_{\pi'} \left[\sum_{t=1}^T \sum_{i=1}^N f' \left(\frac{D_\pi(z_i)}{D_{\text{preference}}(z_i)} \right) a_i(t) \right].
\end{aligned} \tag{27}$$

Therefore, we have

$$\begin{aligned}
J_\lambda(\pi') &\approx \lambda \mathbb{E}_{\pi'} \left[\sum_{t,i} R_{\text{base},i}(s_i(t), a_i(t)) \right] - (1-\lambda) \left[\text{const} + \frac{1}{BT} \mathbb{E}_{\pi'} \left[\sum_{t,i} f' \left(\frac{D_\pi(z_i)}{D_{\text{preference}}(z_i)} \right) a_i(t) \right] \right] \\
&= \mathbb{E}_{\pi'} \left[\sum_{t,i} \left(\lambda R_{\text{base},i}(s_i(t), a_i(t)) - \frac{1-\lambda}{BT} f' \left(\frac{D_\pi(z_i)}{D_{\text{preference}}(z_i)} \right) a_i(t) \right) \right] + \text{const.}
\end{aligned} \tag{28}$$

Define shaped reward as

$$R_h(z_i) = -\frac{1-\lambda}{\lambda BT} f' \left(\frac{D_\pi(z_i)}{D_{\text{preference}}(z_i)} \right).$$
 \tag{29}

Then, we have

$$\begin{aligned}
J_\lambda(\pi') &\propto \mathbb{E}_{\pi'} \left[\sum_{t,i} (\lambda R_{\text{base},i}(s_i(t), a_i(t)) + \lambda R_h(z_i) a_i(t)) \right] \\
&= \lambda \mathbb{E}_{\pi'} \left[\sum_{t,i} (R_{\text{base},i}(s_i(t), a_i(t)) + R_h(z_i) a_i(t)) \right] \\
&= \lambda \mathbb{E}_{\pi'} \left[\sum_{t,i} R_{\text{shaped},i}(s_i(t), a_i(t), z_i) \right],
\end{aligned} \tag{30}$$

where

$$R_{\text{shaped},i}(s, a, z_i) = \begin{cases} R_{\text{base},i}(s, a) + R_h(z_i) & \text{if } a = 1 \\ R_{\text{base},i}(s, a) & \text{if } a = 0. \end{cases} \quad (31)$$

This completes the proof that the scalarized multi-objective problem is equivalent to optimizing a single objective with appropriately shaped rewards.

B.3 Proof of Theorem 7

The proof is structured in three main parts:

1. **Gradient Derivation:** We define the scalarized objective function $J_\lambda(R_h)$ and formally establish the existence of its gradient with respect to R_h .
2. **Stochastic Approximation and ODE Convergence:** We link the discrete, noisy update rule to a continuous-time ODE and show that the iteration asymptotically tracks the ODE's trajectory.
3. **Lyapunov Analysis and Pareto Optimality:** We use a Lyapunov function to prove that the ODE's trajectory converges to its set of stationary points, and we then argue that these points correspond to Pareto optimal solutions of the original bi-objective problem.

Given a shaping reward function R_h , the solver returns the optimal policy by solving the following problem

$$\pi^*(R_h) = \arg \max_{\pi \in \Pi_{\text{feasible}}} \mathbb{E}_\pi \left[\sum_{t=1}^T \sum_{i=1}^N (R_b(s_i(t), a_i(t)) + R_h(z_i)) \right], \quad (32)$$

where $\Pi_{\text{feasible}} = \{\pi : \sum_{i=1}^N a_i(t) \leq B, \forall t\}$. Define the bi-objective function as

$$J(R_h) = (J_1(R_h), J_2(R_h)), \quad (33)$$

where

$$J_1(R_h) = \mathbb{E}_{\pi^*(R_h)} \left[\sum_{t,i} R_{\text{base}}(s_i(t), a_i(t)) \right] \quad (\text{task utility}), \quad (34)$$

$$J_2(R_h) = -C(\pi^*(R_h)) \quad (\text{negative preference violation}). \quad (35)$$

By Theorem 2, the Pareto front can be characterized via weighted scalarization:

$$J_\lambda(R_h) = J_1(R_h) + \lambda J_2(R_h), \quad \lambda \geq 0. \quad (36)$$

Lemma 1. *Under Assumptions (A1)-(A3), $J_\lambda(R_h)$ is differentiable with respect to R_h .*

Proof. By the envelope theorem (Assumption (A1) ensures differentiability):

$$\begin{aligned} \frac{\partial J_1(R_h)}{\partial R_h(z)} &= \mathbb{E}_{\pi^*(R_h)} \left[\sum_{t,i} \mathbf{1}(z_i = z) a_i(t) \right] = BT \cdot D_{\pi^*(R_h)}(z), \\ \frac{\partial J_2(R_h)}{\partial R_h(z)} &= -\frac{\partial C(\pi^*(R_h))}{\partial R_h(z)}. \end{aligned} \quad (37)$$

From the chain rule and Theorem 3,

$$\frac{\partial C(\pi^*(R_h))}{\partial R_h(z)} = \frac{\partial C}{\partial D_\pi(z)} \cdot \frac{\partial D_{\pi^*(R_h)}(z)}{\partial R_h(z)}. \quad (38)$$

Using the implicit function theorem on the optimality condition $\nabla_{\pi} \mathbb{E}_{\pi}[R_{\text{base}} + R_h] = 0$:

$$\frac{\partial D_{\pi^*(R_h)}(z)}{\partial R_h(z)} = \frac{1}{BT} \cdot \text{sensitivity factor.} \quad (39)$$

Therefore, $J_{\lambda}(R_h)$ is differentiable. \square

Lemma 2 (Gradient Formula). *The gradient of J_{λ} with respect to R_h is:*

$$\nabla_{R_h} J_{\lambda}(R_h) = d^{\pi^*(R_h)} - \lambda \nabla_{R_h} C(\pi^*(R_h)) \quad (40)$$

where $d^{\pi^*(R_h)}(z) = BT \cdot D^{\pi^*(R_h)}(z)$ is the expected visitation count.

Proof. It follows

$$\nabla_{R_h} J_{\lambda}(R_h) = \nabla_{R_h} J_1(R_h) + \lambda \nabla_{R_h} J_2(R_h) = d^{\pi^*(R_h)} - \lambda \nabla_{R_h} C(\pi^*(R_h)). \quad (41)$$

\square

The shaping reward function R_h is updated according to the following stochastic approximation (SA) rule:

$$R_h^{k+1} = R_h^k + \eta_k g^k, \quad (42)$$

where η_k is the step-size, satisfying the standard SA conditions: $\sum_k \eta_k = \infty$ and $\sum_k \eta_k^2 < \infty$; $g^k = \hat{\nabla}_{R_h} J_{\lambda}(R_h^k)$ is the stochastic gradient estimate obtained at step k . By Assumption (A3), this feedback $\text{Feedback}^k = f(\delta_U, \delta_D)$ provides a stochastic estimate

$$g^k = \nabla_{R_h} J_{\lambda}(R_h^k) + \xi^k, \quad (43)$$

where $\mathbb{E}[\xi^k | \mathcal{F}_{k-1}] = 0$ and $\mathbb{E}[\|\xi^k\|^2] \leq \sigma^2 < \infty$. The core principle of SA theory is that the long-term behavior of the discrete, noisy iteration is described by a deterministic ODE.

Lemma 3 (ODE Approximation). *Under the standard assumptions on the step-sizes $\{\eta_k\}$ and the noise process $\{\xi^k\}$, the sequence $\{R_h^k\}$ generated by the update rule converges almost surely to the solution set of the following ODE:*

$$\frac{dR_h(t)}{dt} = \nabla_{R_h} J_{\lambda}(R_h(t)). \quad (44)$$

Proof. This is a classical result from the ODE method for analyzing stochastic approximation algorithms [6, 14]. The proof involves showing that the sequence of interpolated processes is tight, and that any of its limit points must satisfy the ODE. The key steps are:

1. *Tightness:* The family $\{\bar{R}_h^n(\cdot)\}$ is tight in $C([0, \infty), \mathbb{R}^d)$;
2. *Characterization of limit points:* Any limit point satisfies the ODE;
3. *Convergence:* By Lyapunov analysis, trajectories converge to the set of stationary points.

\square

Convergence to Stationary Points. We can use the objective function $J_\lambda(R_h)$ itself as a Lyapunov function to analyze the stability of the ODE.

Lemma 4 (Convergence). *The function $J_\lambda(R_h)$ is a Lyapunov function for the dynamics in (44). Consequently, the trajectory $R_h(t)$ converges to the set of stationary points $S = \{R_h : \nabla_{R_h} J_\lambda(R_h) = 0\}$.*

Proof. We examine the time derivative of $J_\lambda(R_h(t))$ along the trajectories of the ODE:

$$\frac{d}{dt} J_\lambda(R_h(t)) = \left\langle \nabla_{R_h} J_\lambda(R_h(t)), \frac{dR_h(t)}{dt} \right\rangle.$$

By the definition of the ODE, $\frac{dR_h(t)}{dt} = \nabla_{R_h} J_\lambda(R_h(t))$, which gives:

$$\frac{d}{dt} J_\lambda(R_h(t)) = \langle \nabla_{R_h} J_\lambda(R_h), \nabla_{R_h} J_\lambda(R_h) \rangle = \|\nabla_{R_h} J_\lambda(R_h)\|^2 \geq 0.$$

This shows that $J_\lambda(R_h(t))$ is monotonically non-decreasing along the trajectories. By LaSalle's Invariance Principle, as $t \rightarrow \infty$, the trajectory $R_h(t)$ must converge to the largest invariant set where the time derivative is zero, which is precisely the set of points where $\nabla_{R_h} J_\lambda(R_h) = 0$. \square

Characterization of Stationary Points.

Lemma 5. *A point R_h^* is stationary for J_λ if and only if it satisfies:*

$$\nabla_{R_h} J_\lambda(R_h^*) = 0 \Leftrightarrow \lambda \nabla_{R_h} J_1(R_h^*) + (1 - \lambda) \nabla_{R_h} J_2(R_h^*) = 0. \quad (45)$$

This is exactly the first-order necessary condition for Pareto optimality in the scalarized problem.

Stationary Points and Pareto Optimality. The final step is to connect the stationary points of the ODE to the desired notion of optimality for the original problem.

Lemma 6 (Optimality). *Assuming the bi-objective problem is convex, if R_h^* is a stationary point (i.e., $\nabla_{R_h} J_\lambda(R_h^*) = 0$ for some $\lambda > 0$), then the corresponding objective vector $(J_1(R_h^*), J_2(R_h^*))$ is a Pareto optimal solution.*

Proof. This is a standard result for the weighted scalarization method. Since $\nabla_{R_h} J_\lambda(R_h^*) = 0$, R_h^* is a (local) maximizer of the scalarized function J_λ . Assume for contradiction that the solution corresponding to R_h^* is not Pareto optimal. Then there must exist another shaping reward \tilde{R}_h such that $J_1(\tilde{R}_h) \geq J_1(R_h^*)$ and $J_2(\tilde{R}_h) \geq J_2(R_h^*)$, with at least one inequality being strict. For any $\lambda > 0$, this would imply:

$$J_\lambda(\tilde{R}_h) = J_1(\tilde{R}_h) + \lambda J_2(\tilde{R}_h) > J_1(R_h^*) + \lambda J_2(R_h^*) = J_\lambda(R_h^*).$$

This contradicts the fact that R_h^* is a maximizer of J_λ . Therefore, the solution must be Pareto optimal. \square

Therefore, we have

$$\lim_{k \rightarrow \infty} (U(\pi^*(R_h^k)), -C(\pi^*(R_h^k))) = (J_1(R_h^*), J_2(R_h^*)) \in \text{Pareto frontier} \quad (46)$$

This completes the proof.

C Additional Results

All experiments are run on a machine with 16GB RAM and M1 chip CPU. The primary bottleneck in speed was the API call limits for using LLM (Gemini Pro). For each experiment, we run 50 independent trials.

C.1 Public Health Domain (ARMMAN)

A public health program managing prenatal care adherence through targeted phone interventions [5, 18].

Environment abstract. We simulate a population of 800 mothers, partitioned into 8 demographic types (each with 100) based on three binary features: **Income:** Low / High; **Education:** Low / High; **Age:** Young / Old. The state of each mother is binary: $s_i(t) \in \{0, 1\}$, where $s_i(t) = 0$ indicates disengagement with health services (high risk), and $s_i(t) = 1$ indicates engagement (low risk). At each round, the planner is allowed to intervene with up to $B = 400$ mothers (i.e., 50% of the total population). Each mother evolves as a controlled MDP associated with a transition kernel and base reward.

Table 3: System Parameters

Parameter	Value
Number of patients (N)	800 pregnant women
Budget constraint (B)	400 calls per round
Time horizon (T)	50 weeks (pregnancy duration)
State space	$\mathcal{S} = \{0, 1\}$ $s = 0$: Non-adherent (high risk) $s = 1$: Adherent (low risk)

Patient Features $z_i = (\text{age}_i, \text{education}_i, \text{income}_i)$:

- Age: $\{1, 2\}$ (Young, Old)
- Education level: $\{1, 2\}$ (Low, High)
- Income level: $\{1, 2\}$ (Low, High)

Base reward function. $R_b(s = 0) = 0.2, R_b(s = 1) = 0.8$.

C.1.1 Transitions

We list the 8 types of transition below

Type 1: High Income High Education High Age

From State 0 with No Call: \rightarrow Stay in State 0: 0.900 \rightarrow Move to State 1: 0.100

From State 0 with Call: \rightarrow Stay in State 0: 0.350 \rightarrow Move to State 1: 0.650

From State 1 with No Call: \rightarrow Stay in State 1: 0.500 \rightarrow Move to State 0: 0.500

From State 1 with Call: \rightarrow Stay in State 1: 0.950 \rightarrow Move to State 0: 0.050

Type 2: High Income High Education Low Age

From State 0 with No Call: \rightarrow Stay in State 0: 0.900 \rightarrow Move to State 1: 0.100

From State 0 with Call: \rightarrow Stay in State 0: 0.250 \rightarrow Move to State 1: 0.750

From State 1 with No Call: \rightarrow Stay in State 1: 0.400 \rightarrow Move to State 0: 0.600

From State 1 with Call: → Stay in State 1: 0.950 → Move to State 0: 0.050

Type 3: High Income Low Education High Age

From State 0 with No Call: → Stay in State 0: 0.900 → Move to State 1: 0.100

From State 0 with Call: → Stay in State 0: 0.500 → Move to State 1: 0.500

From State 1 with No Call: → Stay in State 1: 0.500 → Move to State 0: 0.500

From State 1 with Call: → Stay in State 1: 0.900 → Move to State 0: 0.100

Type 4: High Income Low Education Low Age

From State 0 with No Call: → Stay in State 0: 0.900 → Move to State 1: 0.100

From State 0 with Call: → Stay in State 0: 0.400 → Move to State 1: 0.600

From State 1 with No Call: → Stay in State 1: 0.400 → Move to State 0: 0.600

From State 1 with Call: → Stay in State 1: 0.900 → Move to State 0: 0.100

Type 5: Low Income High Education High Age

From State 0 with No Call: → Stay in State 0: 0.800 → Move to State 1: 0.200

From State 0 with Call: → Stay in State 0: 0.250 → Move to State 1: 0.750

From State 1 with No Call: → Stay in State 1: 0.400 → Move to State 0: 0.600

From State 1 with Call: → Stay in State 1: 0.900 → Move to State 0: 0.100

Type 6: Low Income High Education Low Age

From State 0 with No Call: → Stay in State 0: 0.800 → Move to State 1: 0.200

From State 0 with Call: → Stay in State 0: 0.150 → Move to State 1: 0.850

From State 1 with No Call: → Stay in State 1: 0.300 → Move to State 0: 0.700

From State 1 with Call: → Stay in State 1: 0.900 → Move to State 0: 0.100

Type 7: Low Income Low Education High Age

From State 0 with No Call: → Stay in State 0: 0.800 → Move to State 1: 0.200

From State 0 with Call: → Stay in State 0: 0.400 → Move to State 1: 0.600

From State 1 with No Call: → Stay in State 1: 0.400 → Move to State 0: 0.600

From State 1 with Call: → Stay in State 1: 0.800 → Move to State 0: 0.200

Type 8: Low Income Low Education Low Age

From State 0 with No Call: → Stay in State 0: 0.800 → Move to State 1: 0.200

From State 0 with Call: → Stay in State 0: 0.300 → Move to State 1: 0.700

From State 1 with No Call: → Stay in State 1: 0.300 → Move to State 0: 0.700

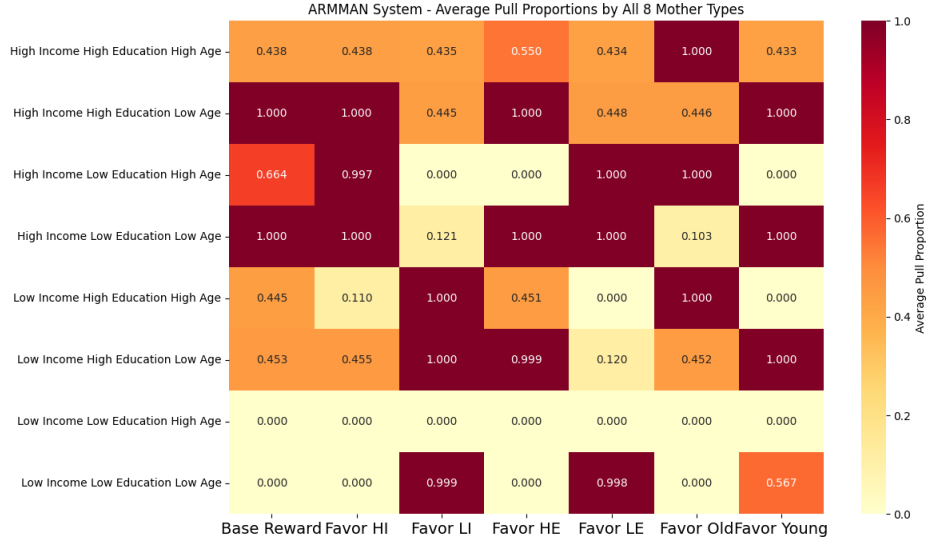


Figure 10: Heatmap for arm-pull proportions under each preference requirement for the public health domain.

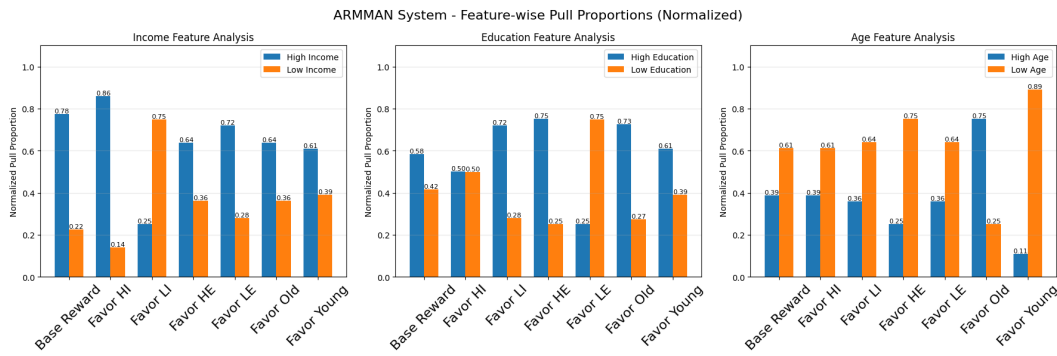


Figure 11: Feature-wise pull proportions for the public health domain.

From State 1 with Call: \rightarrow Stay in State 1: 0.800 \rightarrow Move to State 0: 0.200

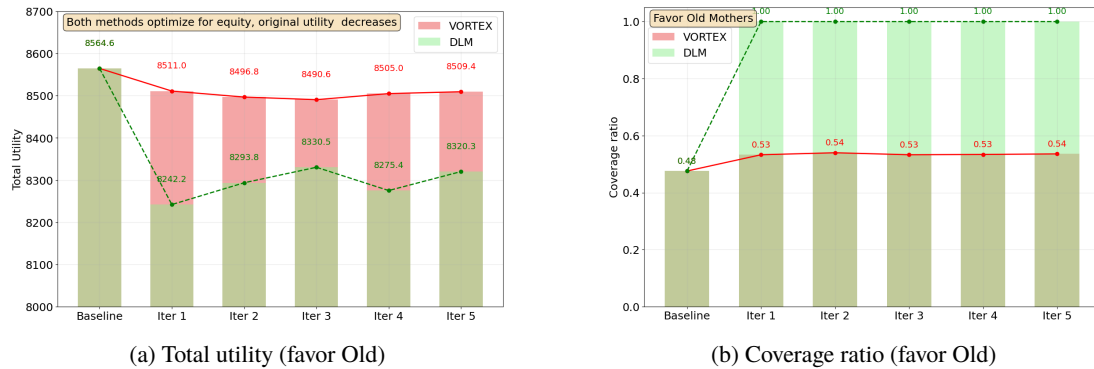


Figure 12: Comparison with DLM for public health domain when preference is favoring old mothers.

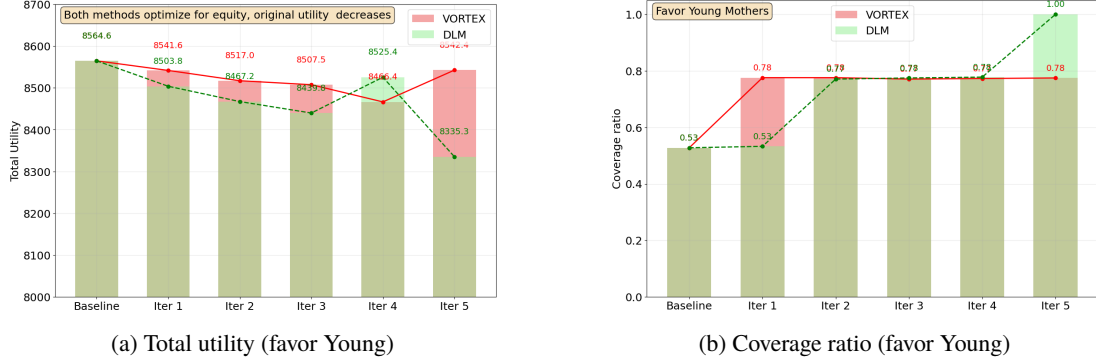


Figure 13: Comparison with DLM for public health domain when preference is favoring young mothers.

C.2 Results for Conservation Domain

An environmental agency is managing anti-poaching patrols in a national park. The goal is to allocate a limited number of ranger teams to different areas to keep the areas secure and protect wildlife [24].

Environment abstract. We simulate a park of 400 patrol areas, partitioned into 4 distinct types (each with 100 areas) based on two binary features: Animal Density: Low / High; Access Difficulty: Low / High. The state of each area is binary: $s_i(t) \in \{0, 1\}$, where $s_i(t) = 0$ indicates the area is "At Risk" (e.g., signs of poacher activity), and $s_i(t) = 1$ indicates it is "Secure". At each round, the agency can deploy ranger teams to patrol up to $B=100$ areas (i.e., 25% of the total park). Each area evolves as a controlled MDP associated with a transition kernel and base reward.

Table 4: System Parameters for Conservation

Parameter	Value
Number of areas (N)	400 patrol areas
Budget constraint (B)	100 patrols per round
Time horizon (T)	52 weeks (one year)
State space	$S = \{0, 1\}$ $s = 0$: At Risk $s = 1$: Secure

Area Features $z_i = (\text{density}_i, \text{difficulty}_i)$:

- Animal Density: 1,2 (Low, High)
- Access Difficulty: 1,2 (Low, High)

Base reward function. $R_b(s = 0) = 0.1, R_b(s = 1) = 0.9$.

C.2.1 Transitions

We list the 4 types of transition below.

Type 1: High Density, High Difficulty

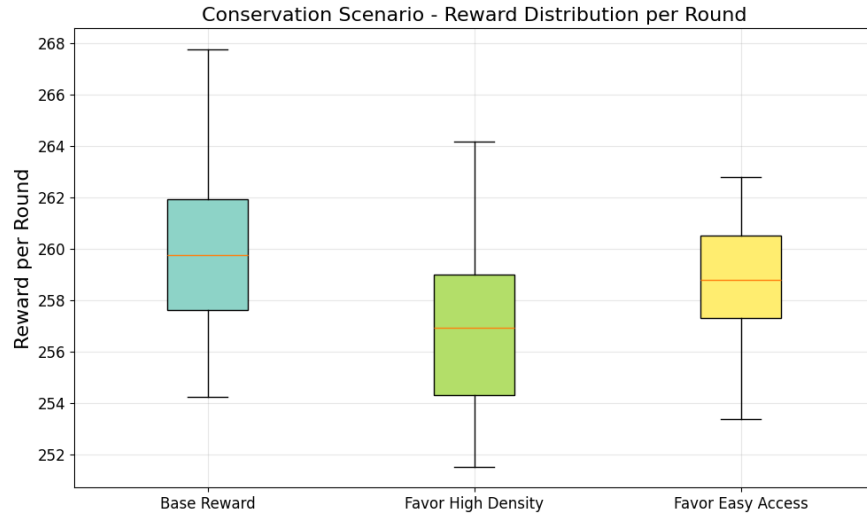


Figure 14: Reward distribution for conservation domain.

From State 0 (At Risk) with No Patrol: \rightarrow Stay in State 0: 0.850 \rightarrow Move to State 1: 0.150

From State 0 (At Risk) with Patrol: \rightarrow Stay in State 0: 0.300 \rightarrow Move to State 1: 0.700

From State 1 (Secure) with No Patrol: \rightarrow Stay in State 1: 0.650 \rightarrow Move to State 0: 0.350

From State 1 (Secure) with Patrol: \rightarrow Stay in State 1: 0.950 \rightarrow Move to State 0: 0.050

Type 2: High Density, Low Difficulty

From State 0 (At Risk) with No Patrol: \rightarrow Stay in State 0: 0.850 \rightarrow Move to State 1: 0.150

From State 0 (At Risk) with Patrol: \rightarrow Stay in State 0: 0.150 \rightarrow Move to State 1: 0.850

From State 1 (Secure) with No Patrol: \rightarrow Stay in State 1: 0.550 \rightarrow Move to State 0: 0.450

From State 1 (Secure) with Patrol: \rightarrow Stay in State 1: 0.950 \rightarrow Move to State 0: 0.050

Type 3: Low Density, High Difficulty

From State 0 (At Risk) with No Patrol: \rightarrow Stay in State 0: 0.900 \rightarrow Move to State 1: 0.100

From State 0 (At Risk) with Patrol: \rightarrow Stay in State 0: 0.400 \rightarrow Move to State 1: 0.600

From State 1 (Secure) with No Patrol: \rightarrow Stay in State 1: 0.800 \rightarrow Move to State 0: 0.200

From State 1 (Secure) with Patrol: \rightarrow Stay in State 1: 0.950 \rightarrow Move to State 0: 0.050

Type 4: Low Density, Low Difficulty

From State 0 (At Risk) with No Patrol: \rightarrow Stay in State 0: 0.900 \rightarrow Move to State 1: 0.100

From State 0 (At Risk) with Patrol: \rightarrow Stay in State 0: 0.250 \rightarrow Move to State 1: 0.750

From State 1 (Secure) with No Patrol: \rightarrow Stay in State 1: 0.700 \rightarrow Move to State 0: 0.300

From State 1 (Secure) with Patrol: \rightarrow Stay in State 1: 0.950 \rightarrow Move to State 0: 0.050

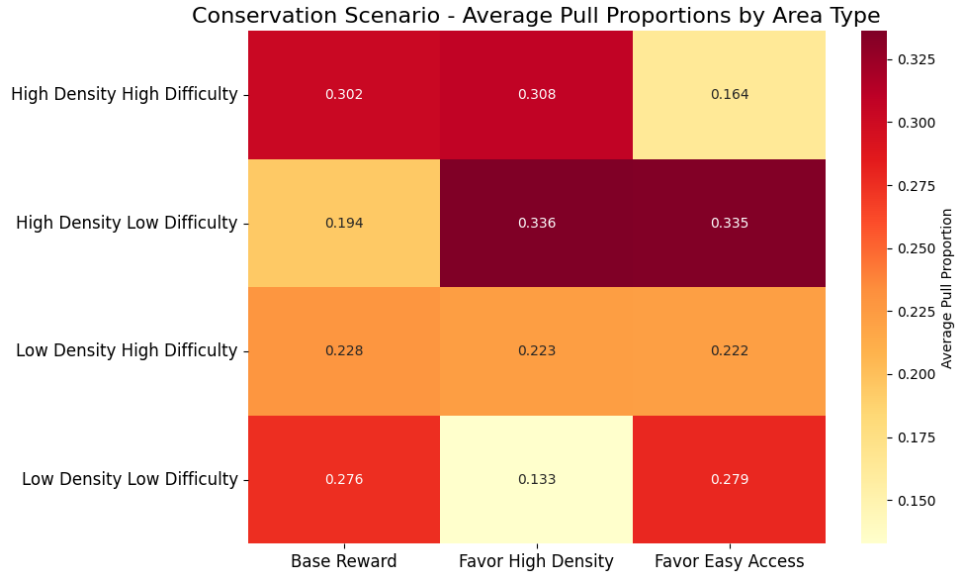


Figure 15: Heatmap for arm-pull proportions under each preference requirement for conservation domain.

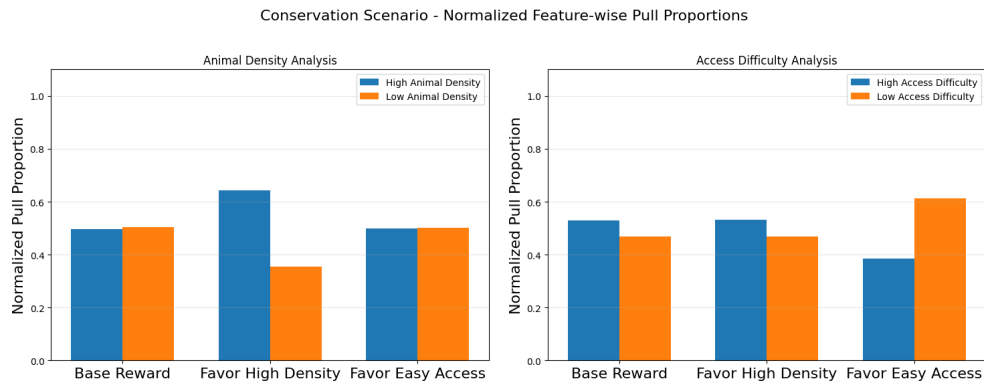


Figure 16: Feature-wise pull proportions under each preference requirement for conservation domain.

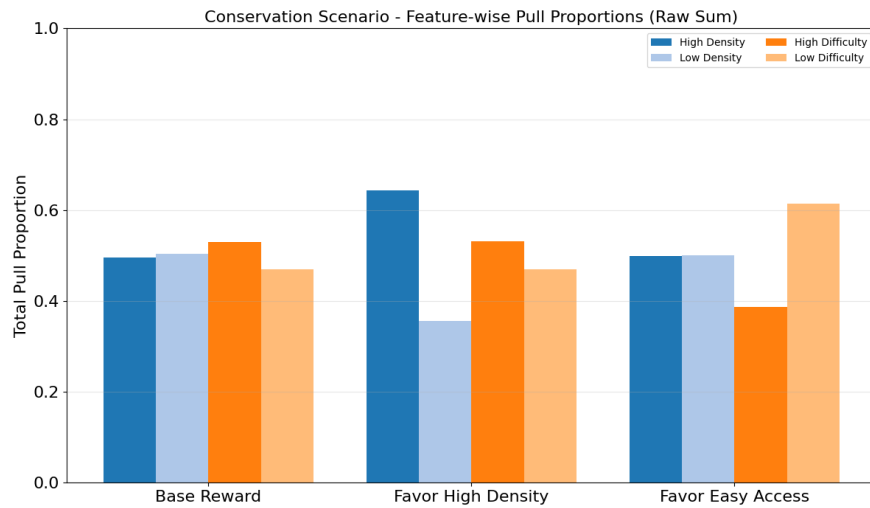
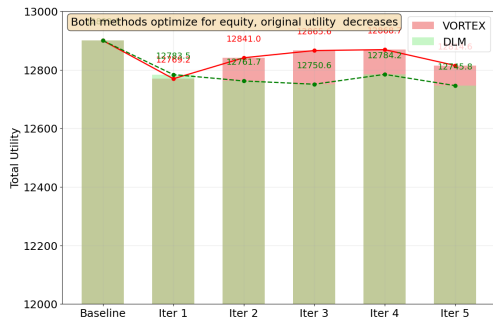
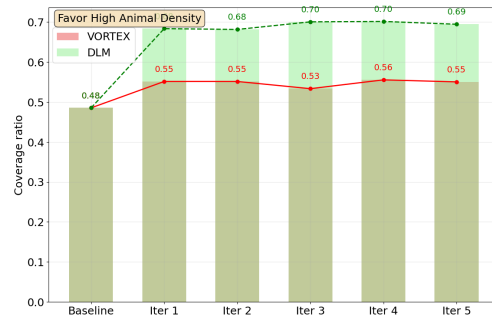


Figure 17: Coverage ratio comparison for conservation domain.

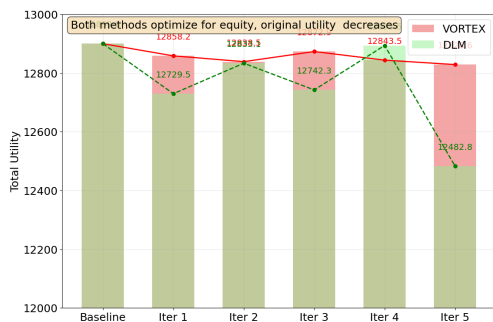


(a) Total utility (favor High Animal Density)

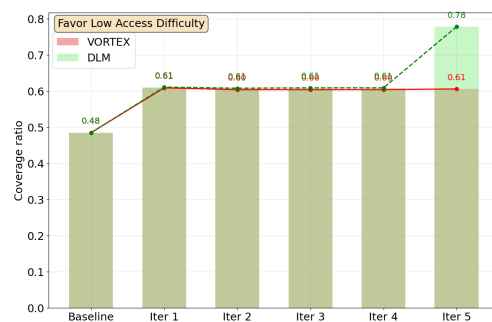


(b) Coverage ratio (favor High Animal Density)

Figure 18: Comparison with DLM for conservation when preference is favoring High Animal Density.



(a) Total utility (favor Low Access Difficulty)



(b) Coverage ratio (favor Low Access Difficulty)

Figure 19: Comparison with DLM for conservation when preference is favoring Low Access Difficulty.